Tikrit Journal of Engineering Sciences (2025); 32(1): 1894
DOI: http://doi.org/10.25130/tjes.32.1.27

IRAQI Academic Scientific Journals

ISSN: 1813-162X (Print); 2312-7589 (Online)

Tikrit Journal of Engineering Sciences

available online at: http://www.tj-es.com

TJES Tikrit Journal of Engineering Sciences

Preparation and Characterization of MgO/Fe3O4 Activated Carbon with Statistically Optimization for Oil Uptake from Emulsion

Ataa Wejood Ali [a], *Nawras Jameel Jassim* [*b], *Mohammed N. Fares* [a]

a Chemical Engineering Department, College of Engineering, Basrah University, Basrah, Iraq.
b Department of Chemical and Petrochemical Techniques Engineering, Basra Engineering Technical College, Southern Technical University, Basra, Iraq.

Keywords:
Metals; Surface; Taguchi; Ultrasonic power; Optimal; Oil adsorption; Produced water.

Highlights:

- *Assisted Ultrasonic Radiation.*
- *Optimization of (MgO/Fe3O4/AC) Preparation.*
- *Analysis of BET Surface Area.*

ARTICLE INFO

Article history:

Received	26 Nov. 2023
Received in revised form	18 Dec. 2023
Accepted	05 Feb. 2024
Final Proofreading	01 Mar. 2025
Available online	28 Mar. 2025

Citation: Ali AW, Jassim NJ, Fares MN. **Preparation and Characterization of MgO/Fe3O4 Activated Carbon with Statistically Optimization for Oil Uptake from Emulsion**. *Tikrit Journal of Engineering Sciences* 2025; **32**(1): 1894.
http://doi.org/10.25130/tjes.32.1.27

*Corresponding author:

Nawras Jameel Jassim

Department of Chemical and Petrochemical Techniques Engineering, Basra Engineering Technical College, Southern Technical University, Basra, Iraq.

Abstract: This novel study objective is to utilize Taguchi experimental design to investigate the optimal preparation parameters of the MgO/Fe3O4/ functionalized activated carbon (MgO/Fe3O4/AC) by modified coprecipitation method aided by ultrasonication. The parameters and their levels were coprecipitation pH (8-10), ultrasonic power (195-455) Watt, and precursors loading wt.% of metals salts (33.4-66) %. The prepared carbon supported with magnetic metals oxides was used as a direct and new step to remove oil from oil/water emulsion, dominating Basra's oil and gas industry pollutants. The study examines the effects of various factors, surface morphology changes, and modifications on the performance of batch adsorption of diesel drops from synthetically oil/water emulsion. The significant parameters for experimental design response were recognized from the regression analysis. The optimal preparation conditions for (MgO/Fe3O4/AC) for adsorption of diesel drops from oil/water emulsion were achieved using a pH of 10, 325watt ultrasonic power, and 50% precursor loading. The outcomes gave evidence of the capacity of the MgO/Fe3O4/AC to remove diesel drops, and the adsorption capacity of the adsorbent has been influenced by coprecipitation preparation parameters. The results showed that 54.8 mg/g of diesel adsorption capacity was achieved at statistically optimized parameters. Characterization methods included FESEM, EDS, and FTIR. The resulting (MgO/Fe3O4/AC) had a BET surface area of 345 m^2/g. The experimentally measured correlation coefficient of 0.999 was found to agree with the expected values from the model strongly.

دراسة عوامل التحضير الأمثل للكاربون المنشط المدعم MgO/Fe3O4 ودراسة قابليتها لامتزاز النفط من المستحلب

عطاء وجود علي[١]، نورس جميل جاسم[٢]، محمد ناصر فارس[١]

[١] قسم الهندسة الكيميائية / كلية الهندسة/ جامعة البصرة / البصرة – العراق.

[٢] قسم تقنيات الهندسة الكيميائية والبتروكيميائية /الكلية التقنية الهندسية/ الجامعة التقنية الجنوبية / البصرة – العراق.

الخلاصة

الهدف من هذه الدراسة الجديدة هو استخدام التصميم التجريبي لتا كوتشي لدراسة العوامل المؤثرة على عملية التحضير المثلى للكربون المنشط (MgO/Fe3O4/AC)عن طريق طريقة الترسيب المعدلة بمساعدة الموجات فوق الصوتية. وكانت العوامل والمستويات المغطاة في حيز الدراسة هي الرقم الهيدروجيني للترسيب (٨-١٠)، وطاقة الموجات فوق الصوتية (١٩٥-٤٥٥) واط ونسبة التحميل الوزنية لأملاح المعادن (٣٣,٤-٦٦). تم استخدام الكربون المحضر المدعم بأكاسيد المعادن في خطوة مباشرة وجديدة لإزالة الديزل التي تهيمن على الملوثات الناتجة عن صناعة النفط والغاز في البصرة. يركز الفحص الكامل على تأثيرات هذه العوامل، بالإضافة إلى التغيرات في شكل السطح على أداء سعة الامتزاز للزيوت والشحوم (O&G) من نموذج مياه ملوث تم التعرف على العوامل الهامة لاستجابة التصميم التجريبي من تحليل الانحدار. تم الحصول على ظروف التحضير المثالية لتحضير (MgO/Fe3O4/AC)باستخدام الرقم الهيدروجيني ١٠، وقوة الموجات فوق الصوتية البالغة ٣٢٥ وات ونسبة التحميل ٥٠٪ بالوزن مما يؤدي إلى سعة امتزاز O&G تبلغ ٥٥ مجم/مجم. تم استخدام المجهر الإلكتروني الماسح (SEM)، EDS ومطياف الأشعة تحت الحمراء (FTIR) لوصف (MgO/Fe3O4/AC) المحضر بشكل أكبر في ظل الظروف المثالية. تم تحديد مساحة سطح BET لـ Fe3O4/MgO/AC من خلال تحليل بيانات امتصاص النيتروجين ضمن نطاق الضغط النسبي من ٠ إلى ١. أظهر (MgO/Fe3O4/AC) الناتج مساحة سطح BET قدرها ٣٤٥ م٢/جم. وقد وجد أن معامل الارتباط المقاس تجريبياً والبالغ ٠,٩٩٩ يتفق بشدة مع القيم المتوقعة من النموذج.

الكلمات الدالة: المعادن، السطح، تاجوتشي، الطاقة فوق الصوتية، الأمثل، امتصاص الزيت، المياه المنتجة

1.INTRODUCTION

Substantial quantities of wastewater are produced due to oil and gas activities, commonly known as "produced water" (PW). It is essentially a mix of the water that is naturally trapped in a well and the water injected in desalters as a part of the surface operations for improved oil and gas recovery [1]. The composition of produced waters (PWs) is intricate and diverse, irrespective of the extraction location and geological circumstances. They contain a mixture of dissolved and suspended constituents, including oil, solid particles, dissolved gases, and inorganic and organic compounds [2]. Treatment of produced water is crucial because of environmental authorities' regulatory restrictions, which constitute a global problem due to the rising volume of waste to more than three times the volume of oil production. Before being discharged or injected into reservoirs, generated water from oil and gas activities must first undergo various treatments mandated by environmental standards to minimize formation damage [3]. Production project operators have implemented various independent and integrated treatment procedures involving physical, biological, and chemical methods for the produced water treatment and reuse [4]. Several strategies have been employed to treat water contaminated with oil and hydrocarbons. However, adsorption has garnered significant interest due to its non-destructive approach to removing these pollutants. This method offers a low-cost solution with excellent efficiency and simplicity. The operation is conducted to ensure minimal environmental impact and does not result in any secondary contamination. The literature reported that the adsorption treatment operates at low concentrations with less process time and much lower cost than other treatment methods. Lowering the treatment cost allows PW to be reused in several applications [5, 1]. One additional benefit of the adsorption process is its capacity for regenerating the adsorbent material, which can be accomplished through heat regeneration or chemical eluents to facilitate desorption [6]. Various adsorbents have been investigated to effectively remove oil and hydrocarbon from produced water, exhibiting notable absorption capabilities [7-12]. Utilizing adsorbents composed of activated carbon has emerged as a highly effective approach for water treatment due to its cost-effectiveness and high removal capacity [7, 13, 14]. Activated carbon is widely recognized as a highly effective adsorbent in wastewater treatment, which is primarily attributed to its remarkable adsorption capacity, expansive surface area, significant surface reactivity, and cost-effectiveness [15]. Utilizing carbon materials as a precursor for producing activated carbon is of utmost importance. There is a wide range of potential sources for these, including petroleum coke, wood, coal, polymers, and various types of biomass such as coconut shells, seeds, sawdust, chitosan, and rice husks [16]. Among these options, coconut shell waste stands out due to its abundance, renewable nature, and exceptional adsorption capabilities [17]. Many studies have investigated the potential use of activated carbon to adsorb various target contaminants from produced water [18, 19, 13, 10]. Producing activated carbonaceous materials includes several procedures and treatments, leading to the development of a complex material that typically has significant potential for eliminating specific pollutants [20].

Meanwhile, using magnetic particles shows potential in enhancing the adsorption capabilities of activated carbon, enabling its efficient separation from the liquid by applying an external magnetic field [21]. On the other hand, due to their large surface area, activated carbon with metal oxides exhibits exceptional physical adsorption capabilities. Furthermore, the metal oxide possesses a wide range of active sites, enabling it to show significant chemical adsorption capabilities [22]. Numerous studies have shown using metal oxide/activated carbon (AC) composites to remove contaminants and explore their various adsorption mechanisms [23-25]. The present work investigates the performance of a novel ($MgO/Fe_3O_4/AC$) adsorbent prepared using the coprecipitation-ultrasonic method for oil and grease adsorption from simulated produced water. This work is reporting for the first time the effect of coprecipitation-ultrasonic process parameters such as coprecipitation pH, ultrasonic power, and precursors loading wt.% of metals salts on O&G adsorption capacity. The Taguchi method, using an L_9 array design, was employed to optimize the process parameters using a statistical experimental design. In addition, the synthesized (MgO/Fe3O4/AC) were characterized using Scanning electron microscopy (SEM), EDS, infrared spectroscopy (FTIR), and Brunauer–Emmett–Teller (BET) surface area methods. This topic is a foundation for conducting a subsequent study to explore the application of MgO/Fe3O4 Activated Carbon for adsorption oil from actual water produced in batch and continuous processes.

2.MATERIAL AND METHODS

2.1.Materials

Coconut shells collected from local markets in Basrah were used as precursors to produce activated carbon. Ferric chloride Hexahydrate ($FeCl_3.6H_2O$) (Thomas Baker) and Magnesium chloride hexahydrate $MgCl_2.6H_2O$ (Magnesia) were used as the precursor's salts for the synthesis of Fe_3O_4 and MgO nanoparticles. Sodium hydroxide pellets (Romil), HCl (37%) (Scharlau), distilled water, ethanol (99% purity) (Honeywell) as a solvent, H_3PO_4 60% (v/v), and diethylene glycol 99.5% purity (Carlo Erba) were used in the present investigation. A diesel sample was obtained from a petrol station, which was selected as the model fuel to form the emulsion. The stock emulsion with an oil concentration of 114 ppm was prepared by homogenizing 1 vol.% of diesel with 99 vol% distilled waters at room temperature. The emulsion was homogenized using ultrasonic power (600 Watt) for one hour. The produced stable emulsion was then examined to measure the oil concentration in water and used to conduct the adsorption experiments.

2.2.Preparation of Activated Carbon

The raw coconut shells were cleaned and dried at 80 °C overnight. In the carbonization stage, the cleaned biomass (565g) was charged to a furnace reactor Vecstar (UK), and the pyrolysis reaction was performed at a temperature of 600°C for 2 hours at a rate of 4 °C/min. The reaction conditioning with nitrogen gas flow was 2 L/min. The impregnation step was conducted by soaking carbon produced with H3PO4 acid at an impregnation ratio of 2:1 for 4 hours and continuously stirring. The produced activated carbon was then dried at 80 °C overnight; the activated carbon was then subjected to reactivation at the furnace reactor at a temperature of 650 °C for 2 hours under continuous nitrogen flow. The activated carbon was subsequently rinsed with distilled water until the pH reached a range of 6.5 to 7. The activated carbon, which went through a washing process, was thereafter subjected to oven drying at a temperature of 100°C for 1 hour. The final activated carbon was subjected to crushing and sieving until the particle size reached 300 to 150 µm.

2.2.1.Synthesis of Fe_3O4/MgO Loaded Activated Carbon

The synthesis of Fe_3O4/MgO functionalized activated carbon was syntheses by minor modifications to the methodology outlined in the prior research endeavors [26]. The method was summarized (100 mL) of DEG (diethylene glycol) poured in a 300 ml beaker and heated to 120 °C for one hour, then 5g of NaOH was added, under mixing. The resultant mixture was cooled to 80 °C to prepare a stock solution used to adjust the reaction pH later. A required amount of AC was dispersed in 40 mL of raw DEG in a glass reactor with three necks around the bottom to control temperature, nitrogen flow, and ultrasonic mixing. Different amounts of metal precursor salts were added at a specified wt. % to the reactor under a stream of nitrogen gas. The reaction time was fixed to 30 min, and the temperature was maintained at 80°C. The studded parameters precursors loading wt.%, ultrasonic power, and solution pH changed according to Taguchi's design. The resultant mixture was further cooled and filtered. The produced precipitate was dried in an oven at a temperature of 90°C overnight.

2.3.Experimental Sets

The Taguchi experimental design is a methodology used in the field of engineering and quality management to optimize the performance of a system or process. This methodology effectively minimizes the required experimental configurations and offers an impartial assessment of the control parameters. In this investigation, Taguchi's orthogonal matrix design was employed to determine the best conditions for preparing and producing ($MgO/Fe_3O_4/AC$). The analysis of mean

(ANOVA) and regression analysis were determined by employing Minitab®21 software. The input parameters of experiments, stated in Table 1, were the preparation pH, ultrasonic power, and precursors loading wt.%. Each input parameter had three levels, a total of 9 experiments employed for the L9 Taguchi orthogonal array to optimize the adsorption capacity of diesel from simulated produced water. The larger Taguchi's, the better is adopted (Eq. (1)) to analyze experimental preparation parameters for diesel adsorption capacity.

$$SN_L = -10\log\left(\frac{1}{n}\sum_{i=1}^{n}\frac{1}{Y_i^2}\right) \quad (1)$$

where:
SN_L: Signal-to-noise ratio large.
n: The number of runs.
Y_i: The response of each experiment at the i_{th} run.

2.4.Adsorption Study

Applying ($MgO/Fe_3O_4/AC$) for batch adsorption of oil removal from emulsion was studied. The batch studies involved adding 100 mL of diesel emulsion as simulated produced water, with an initial oil concentration of 114 ppm to 0.2 g of ($MgO/Fe_3O_4/AC$). The adsorption duration was set at 1 hour, accompanied by a mixing velocity of 190 (rpm). The pH of the simulated produced water was adjusted to a neutral value of 7. The oil content of the produced water was determined using the HACH DR6000 instrument. The adsorption capacity of oil (q_e) was determined by Eq. (2):

$$q_e = \frac{(c_i - c_e)*v}{w} \quad (2)$$

where q_e is the amount of oil adsorbed (mg/L), c_i and c_e are the initial and final diesel concentration (mg/l), V is the experimental volume of the solution (L), and W is the weight of (MgO/Fe3O4/AC) used (g). The orthogonal array design of the nine experiments and the investigated response is listed in Table 2.

Table 1 Control Parameters Levels for Preparation of Fe3O4/MgO Functionalized Activated Carbon Process.

Variable	Unit	Min. value	Max. value
pH		8	10
Ultrasonic Power	watt	195	455
Precursors Loading wt.% (based on Mg)	%	33.4	66

Table 2 Taguchi Experiment Design for L9 Orthogonal Array.

Run NO.	pH	Ultrasonic Power (Watt)	Precursors Loading Wt.% based Mg	Adsorption Capacity of oil
1	8	195	50.0	51.600
2	8	325	66.7	52.100
3	8	455	33.4	51.900
4	9	195	66.7	51.550
5	9	325	33.4	54.385
6	9	455	50.0	53.800
7	10	195	33.4	52.315
8	10	325	50.0	54.800
9	10	455	66.7	54.60

2.5.Characterization of Fe3O4/MgO Activated Carbon

2.5.1.FTIR Analysis of (MgO/Fe3O4/AC)

The FTIR approach was used to identify the functional groups on the surface of MgO/Fe3O4 /Ac before and after oil adsorption from the emulsion. The results are displayed in Fig. 1. The infrared (FTIR) spectra were measured in the wavenumber range of 400–4000 cm-1. The C = O vibrations at 1750 and 1743 cm-1 after adsorption suggest the presence of a carbonyl group. The bands at 3445cm-1 in the composite indicated vibrations of O-H stretching, and binding water was typically associated with the stretching vibration of the hydroxyl (-OH) group peaks in the region2856 - 2925 cm-1 were associated. C-H stretching a 1610 cm-1 was associated with C=C. The peak at 498-815 cm-1 could be attributed to the Fe-O and Mg-O (metal-oxygen) bond stretching vibrations [27, 28].

2.5.2. Microstructural Analysis with FESEM

The morphology and particle distribution of (MgO/Fe3O4/AC) was tested in field emission scanning electron micrographs. As shown in Fig. 2 below, the field emission scanning electron micrographs of (MgO/Fe3O4/AC) before oil adsorption were considered. Due to the behavior of the (MgO/Fe3O4) nanoparticles, crust-shaped, spongy magnetic nanoparticles were observed. The (MgO/Fe3O4/AC) micrographs (Fig. 2 (a, b, c)) are seen to be coarser, homogenous, and porous. As a result, the surface morphology of the activated carbon was uniform and comparatively smooth. Each (MgO/Fe3O4) nanoparticle had a size that fell between 10 and 30 nm, consistent with the FE-SEM picture, Figure 2 (b, c), and was found on the surface of the AC. It is evident that the Fe3O4, MgO, and AC were virtually monodispersed and had a mean diameter of 20 nm. The findings of the

Brunauer-Emmett-Teller (BET) test showed that AC had an average pore capacity of 102.34 cm^3/g and a substantial specific surface area of 445.45 m^2/g. However, the presence of Activated Carbon-MgO and Fe_3O_4 changed the properties of Activated Carbon-MgOFe3O4, resulting in a minor decrease in the pore volume and surface area to 79.29 cm^3/g and 345.11 m^2/g, respectively. The findings obtained from the Field Emission Scanning Electron Microscopy (FESEM) analysis of Fig. 3 (a) and (b) demonstrate that the composition of AC underwent modifications subsequent to its compositing with MgO-Fe_3O_4. Additionally, the findings from the EDS study indicated that AC was comprised entirely of carbon, as depicted in Fig. 3 (c). The AC/MgOFe3O4 composite material exhibited the presence of magnesium (Mg), iron (Fe), and oxygen (O) elements. The elemental composition of the composite material was determined to be 36.4% carbon (C), 26.8% oxygen (O), 25.00% iron (Fe), and 11.9% magnesium (Mg), as depicted in Fig. 3 (c). The results suggest that the attachment of MgO and Fe_3O_4 particles to the surface of coconut-activated carbon was successfully achieved.

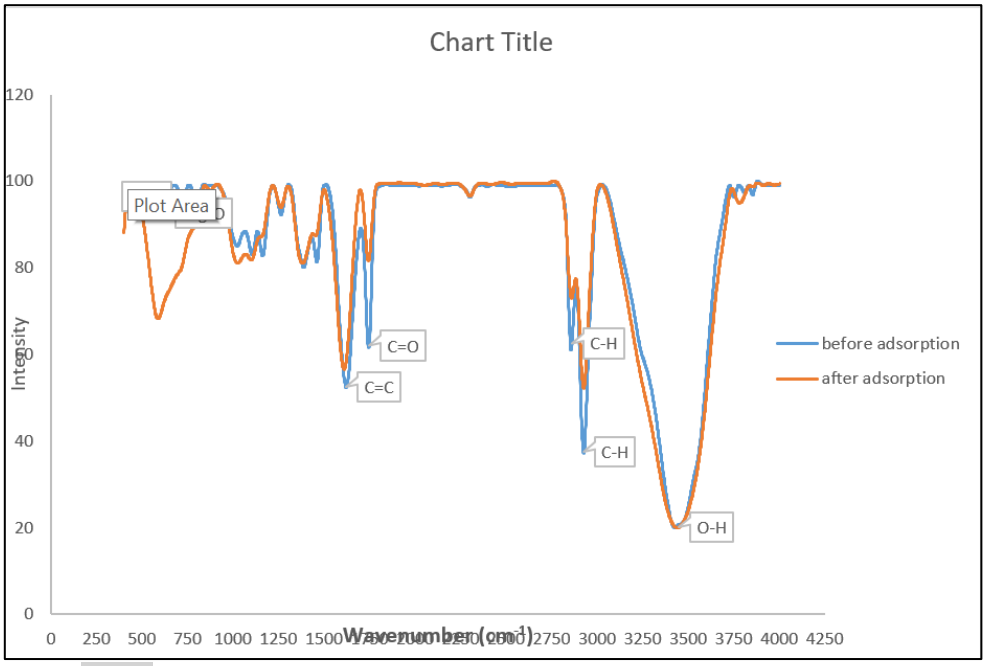

Fig. 1 FTIR Analysis of MgO/Fe_3O_4/AC Before and After Adsorption.

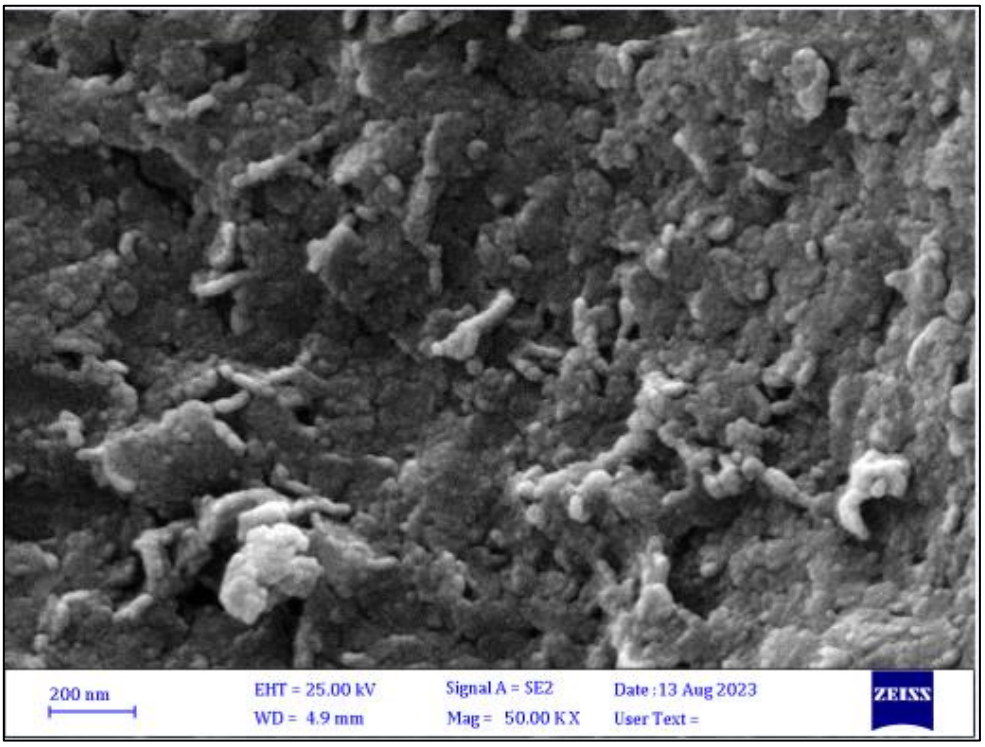

(a)

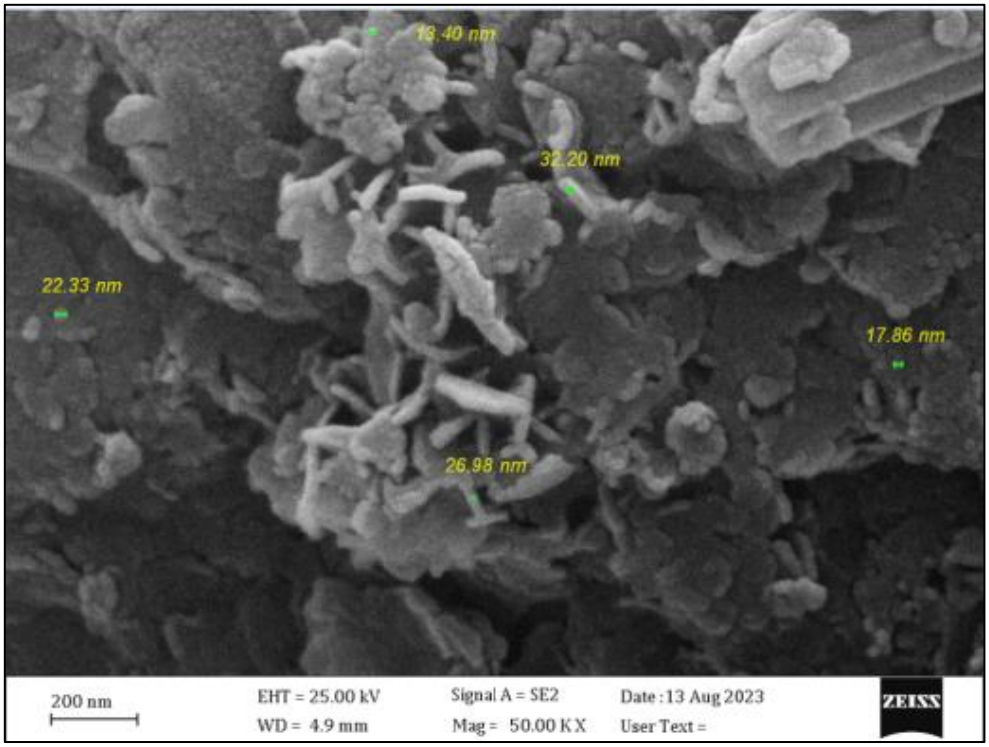

(b)

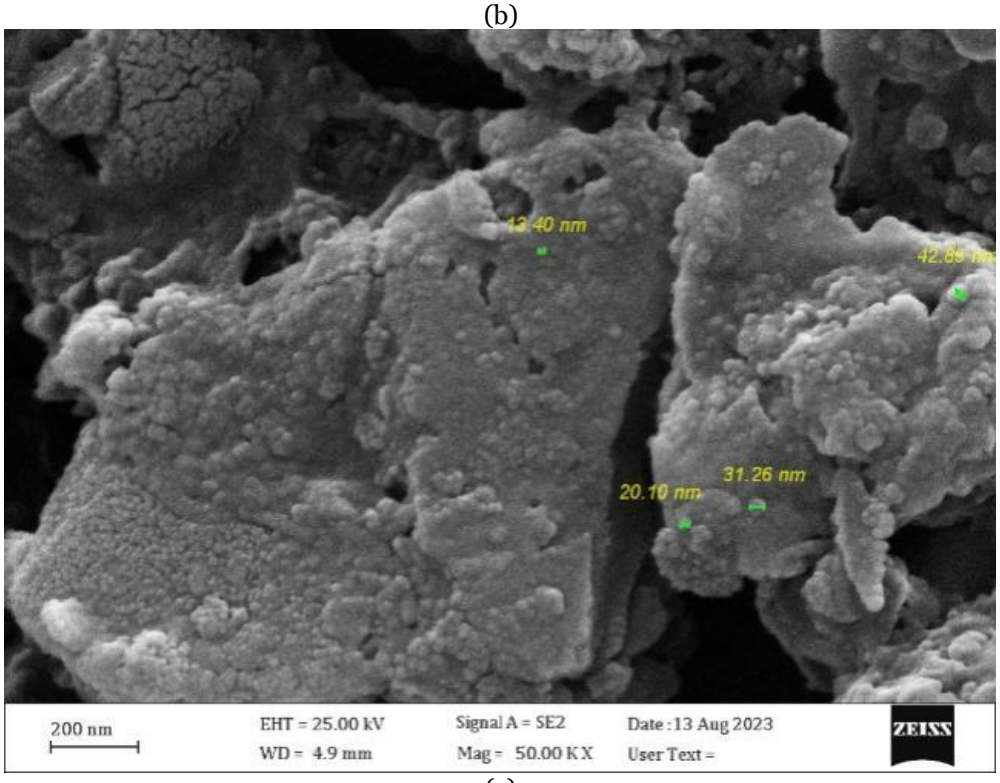

(c)

Fig. 2 FESEM MgO/Fe3O4/AC Nanocomposite (a, b, and c).

Table 3 BET and Total Pore Volume for AC.

	vm **(cm³(STP)/g)**	***aBET*** **(m²/g)**	**Mean pore diameter(nm)**	**Total pore volume(cm³/g)**
AC	102.34	445	1.6803	0.1871
AC/Fe3O4/MgO	79.29	345	1.7923	0.1546

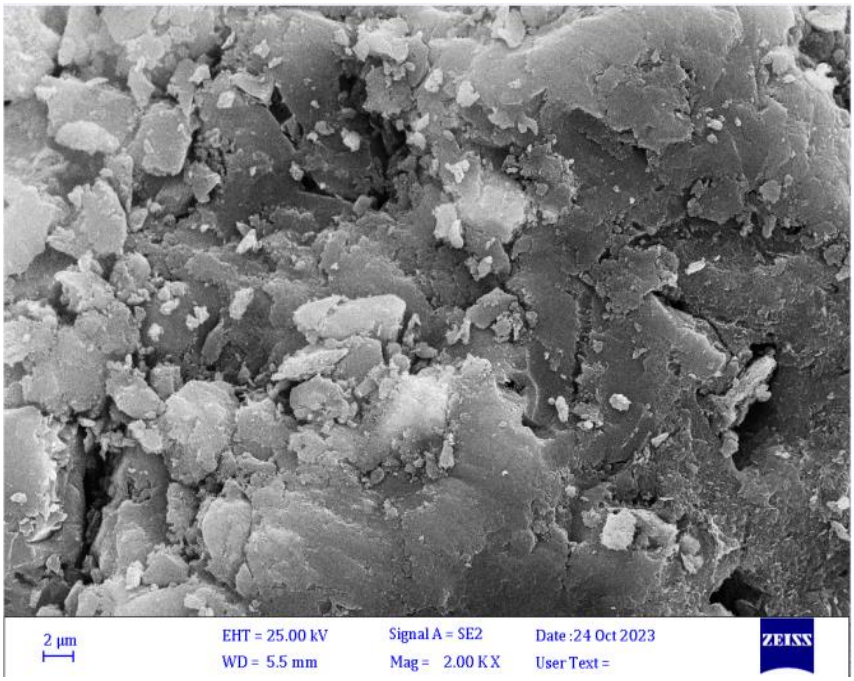

(a)

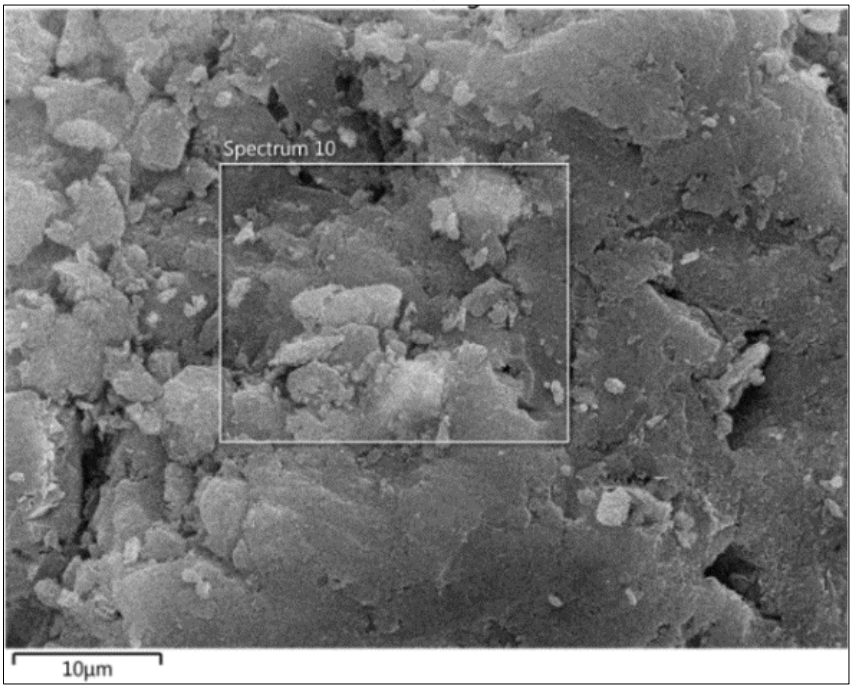

(b)

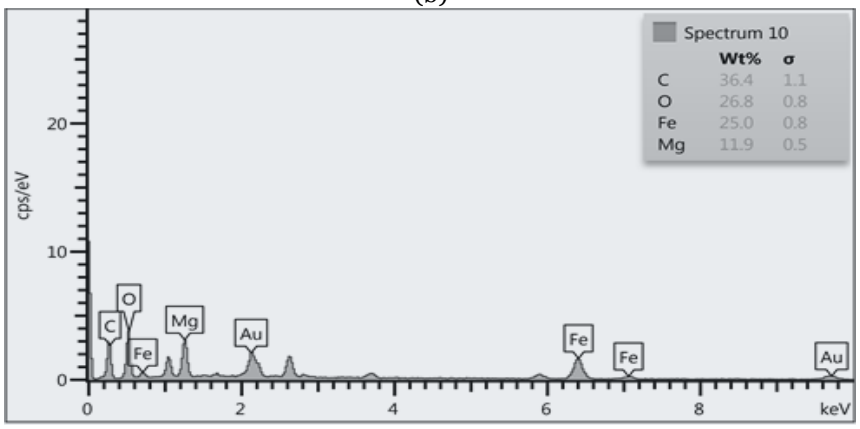

(c)

Fig. 3 FESEM (a and b) and EDS Spectra (c) for (MgO/Fe3O4/AC).

3.RESULTS AND DISCUSSION

3.1.Taguchi Analysis

Three control factors, precursors Loading Wt.%, coprecipitation pH, and ultrasonic power, were tested against oil adsorption capacity as a response in the Taguchi method. The analysis was based on the results noted in Taguchi orthogonal array L_9 runs. The response from L_9 runs listed in (Table 2) were used as the basis for the analysis. It was determined that the higher the S/N ratio, the better. According to the computed S/N ratio, the primary effect diagram is shown in Fig. 4. The primary effect diagram explains how different parameters affect the oil adsorption capacity, as illustrated in Fig. 5. The S/N value was used to control the most significant parameter/s and the contributing level toward maximizing oil adsorption capacity. Table 4 represents the main effect of the three parameters on oil adsorption capacity from Taguchi Analysis of oil Adsorption Capacity mg/g versus pH, Ultrasonic Power (W), and Precursors Loading Wt.%.

Table 4 Response for Means (SN).

Level	pH	Ultrasonic Power (W)	Precursors Loading Wt.%
1	51.87	51.82	52.87
2	53.25	53.76	53.40
3	54.07	53.60	52.92
Delta	2.20	1.94	0.53
Rank	1	2	3

3.1.1.Effect of Ultrasonic Power on Adsorption Capacity

It is clear from Figs. 4 and 5 that the adsorption capacity increased with ultrasonic power, from (195 W) to a maximum value of (325W) power, and then slightly dropped as power was further increased to (455W). At these power levels, the measured adsorption capacities were (51.8, 53.90, and 53.6) mg/g, respectively. The ultrasonic power generates cavitation, creating a microscale bubble in the liquid. The growth, implosive, and collapse of microbubbles in a liquid will generate intense force, causing super mixing. During cavitation, high pressures and temperatures were locally generated, creating turbulence that enhances coprecipitation reactions and deep impregnation of metals oxides in the activated carbon bulk. This effect modifies the structure of metal oxides and activated carbon during the coprecipitation process at increasing power from (195 W) to (325W). At power levels exceeding (325W), a reduction in adsorption capacity occurred due to forming cavity clouds, subsequently reducing the coprecipitation reactions of metal oxides on the surface of activated carbon. Consequently, the adsorptive capacity was diminished to 53.6 mg/g when the power reached (455W) [29].

3.1.2.Effect of pH Coprecipitation on Adsorption Capacity

It can be observed from Figs. 4 and 5 the effect of the pH of the coprecipitation method on the adsorption capacity. As pH increased from value 8 to 10, the adsorption capacity increased from 51.8 to 54.2 mg/g. The increasing pH value affects the surface charge, nucleation, and growth of metal oxide particles during coprecipitation reactions. As a result of increasing pH, the reactions occurred more rapidly, impacting the composite's morphology and distribution of metal oxide particles within the activated carbon matrix. Juang et al., [26] investigated the impact of varying the weight ratio of metal salt to OH groups on the microstructure and adsorption ability of Fe3O4/AC nanocomposites. It was shown that the weight ratios of FeCl3 and NaOH employed significantly influenced the pH of coprecipitation, thereby affecting the microstructure and adsorption capacity of the nanocomposites.

3.1.3.Effect of Precursors Loading Weight %

The last graph in (Figs. 4 and 5) represents the effect of the precursors Loading Wt.% on the activated carbon surface. Figures 4 and 5 clearly indicate the significant difference between MgO: Fe3O4 precursor loading weight % on diesel drops removal capability from emulsion, which proves the composite's excellent performance over Fe3O4: MgO, where the best balance was 50% to mix the metal salts and load them on the activated carbon. This loading ratio is suitable for applying prepared adsorbent for oil and grease adsorption. Figures 4 and 5 illustrate a significant development in the diesel adsorption capacity when the metal salt precursor loading was at 50%. This increase can be attributed to the rise in available adsorption sites and functional groups on the Fe3O4/MgO/AC surface. However, the change in the adsorption capacity was not substantial for the precursor loading wt. (33.4 and 66.7). The possible cause for this could be the agglomeration of the nanocomposite, which may have resulted in a decrease in the accessible surface area for adsorption, indicating that a metal salt with a precursor loading of 50% possesses the necessary quantity of active sites to achieve the highest possible adsorption capacity. These results agree with [9, 27].

3.2.Regression Analysis

The Minitab 21 software conducted an examination independently, computed the impact of each factor at every level, and then, based on the variations it produced, each factor's significance was examined. Table 5 shows the S/N ratio response used for the present investigation. The findings indicated that among the variables, pH was the most effective. Power came as the second factor, and the ratio was the third. The changes in the factors were also noted to impact the adsorption capacity of oil significantly. The

most efficient factors for oil adsorption capacity were identified using the regression analysis technique and coefficient of determination (R^2) in the studied data. The coefficients, including the sum of squares (SS), degrees of freedom (DF), distribution of the ratio (F), mean square (MS), and p-value, are considered in the regression analysis and presented in a typical tabular style. Table 6 displays all of these features together with their mathematical values. The present investigation utilizes the F-ratio to assess the validity of the tested hypothesis. At the same time, the p-value quantifies the degree of compatibility between the data and the null hypothesis. A smaller p-value indicates a more significant amount of evidence against the null hypothesis as a whole.

The regression equation, derived from Minitab 21 software, is shown in Eq. (3). The obtained values for R^2, R^2 adj, and R^2 predicted were 99.99%, 99.96%, and 99.61%, respectively, as shown in Table 6. Therefore, the experimental results exhibited a strong fit with the presented model. The obtained p-value of 0.00 suggests statistical evidence to support the significance of the model. The percentage contribution (PC) values for each parameter were computed and are presented in Table 6. According to Table 6, it can be observed that the parameter pH exhibited the highest level of significance, contributing 43.6% towards the adsorption capacity of oil over the prepared MgO/Fe3O4 Functionalized Activated Carbon, surpassing the contributions of all other parameters.

Oil Adsorption Capacity mg/mg = 35.94 + 3.659 pH – 0.01945 Ultrasonic Power (W) - 0.027433 Precursors Loading Wt.% - 0.2758 pH*pH - 0.000062 Ultrasonic Power (W)*Ultrasonic Power (W) + 0.007411 pH*Ultrasonic Power (W) **(3)**

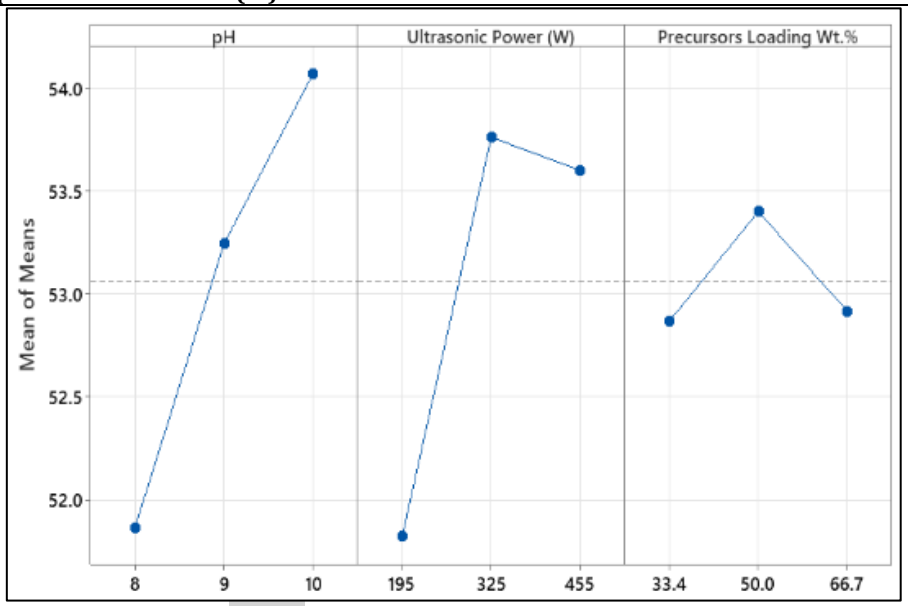

Fig. 4 Main Effect Diagram of Means.

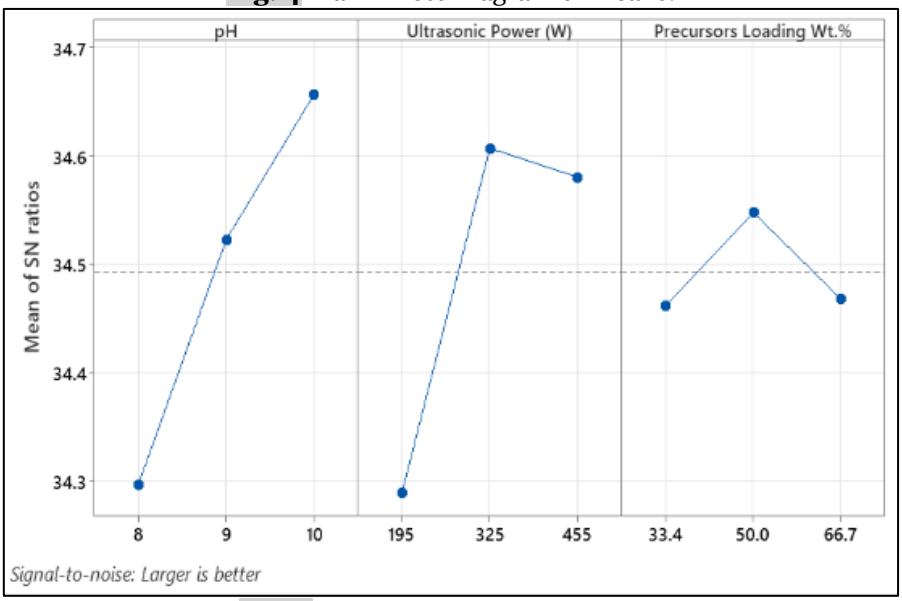

Fig. 5 Main Effect Diagram of SNR.

Table 5 Response for Signal to Noise Ratios (Larger is better).

	pH	Ultrasonic Power (W)	Precursors Loading Wt.%
1	34.30	34.29	34.46
2	34.52	34.61	34.55
3	34.66	34.58	34.47
Delta	0.36	0.32	0.09
Rank	1	2	3

Table 6 Analysis of Variance.

Source	DF	Seq SS	Contribution	Adj SS	Adj MS
Regression	6	16.7245	99.99%	16.7245	2.78742
pH	1	7.2930	43.60%	0.0813	0.08130
Ultrasonic Power (W)	1	4.7437	28.36%	0.1419	0.14193
Precursors Loading Wt.%	1	0.0036	0.02%	0.7833	0.78333
pH*pH	1	0.1522	0.91%	0.1522	0.15217
Ultrasonic Power (W)*Ultrasonic Power (W)	1	2.2085	13.20%	2.2085	2.20850
pH*Ultrasonic Power (W)	1	2.3235	13.89%	2.3235	2.32353
Error	2	0.0018	0.01%	0.0018	0.00090
Total	8	16.7263	100.00%		

Source	F-Value	P-Value
Regression	3103.50	0.000
pH	90.52	0.011
Ultrasonic Power (W)	158.02	0.006
Precursors Loading Wt.%	872.15	0.001
pH*pH	169.42	0.006
Ultrasonic Power (W)*Ultrasonic Power (W)	2458.93	0.000
pH*Ultrasonic Power (W)	2587.00	0.000
Error		
Total		

3.3.Effect of Experimental Parameters on the Adsorption Process

The estimated response model and the impact of coprecipitation reaction preparation parameters are described in Fig. 6 (a, b, c). Analysis of the 3D surface plots suggests that as the pH level increased, the adsorption capacity of diesel also increased, peaking at a pH of 10 in the alkaline medium. The adsorption capacity value rose as power was increased (Fig. 6 (a, b) and reached the maximum value at the mediate limits of 325 Watt. Then, the increasing power decreased the adsorption capacity due to generating intense acoustic cavitation, creating microbubbles and shockwaves in the reaction medium. Additionally, it was found that the effect of the precursors loading wt.% on adsorption capacity value was minimal compared with PH and power (Fig. 6 (b, c)). The impact of different weight percentages (wt.%) of precursors on the adsorption capacity can be noticed in Figure 6 (b, c). Adding metals to activated carbon enhanced its adsorption capacity for diesel due to the increased presence of surface oxygen groups, which in turn leads to the formation of more effective adsorption sites [30]. Adding metal oxides enhances the capacity of adsorbents to absorb more oil. However, if the ratio of oxides exceeds 50%, the adsorption capacity will decrease due to a reduction in surface area. (Kaur et al., 2021) [31] highlighted the significant influence of pH on the oil adsorption capacity, making it the second crucial element in the preparation procedure. The figure clearly demonstrates that the oil adsorption capability increases when the pH of the solution rises from 9 to 11. The pH value is an essential part of the nucleation and aggregation processes that occur during the production of metal oxide particles. Through the increase in pH from 9 to 11, the rate of aggregation exceeded the rate of nucleation, resulting in the complete precipitation of metal oxides and the formation of large-sized particles, precipitating pure loaded metal oxides (MgO/Fe3O4) on the surface of activated carbon, increasing surface roughness and charge to enhance the adsorption capabilities for oil. According to Huang et al., [32], it was discovered that the impact of the weight percentage of precursors on the adsorption capacity is relatively insignificant compared to the effects of pH and power, Figs. 6 (b, c).

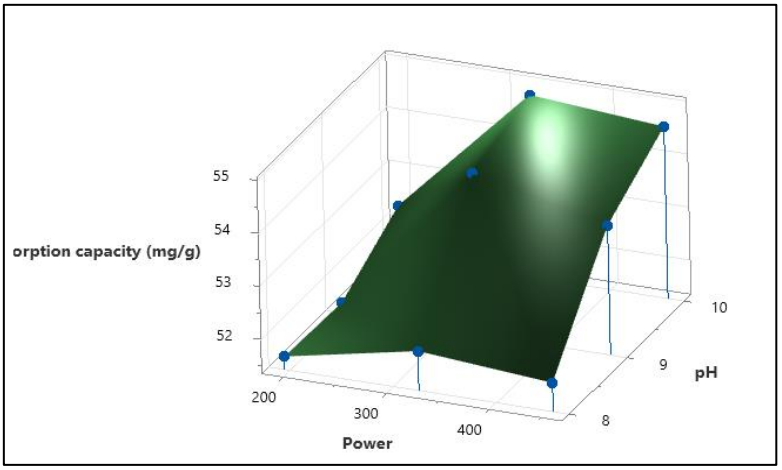

(a)

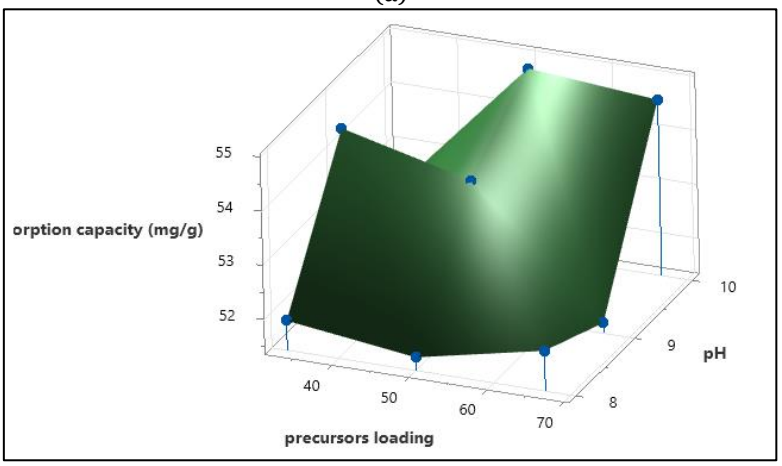

(b)

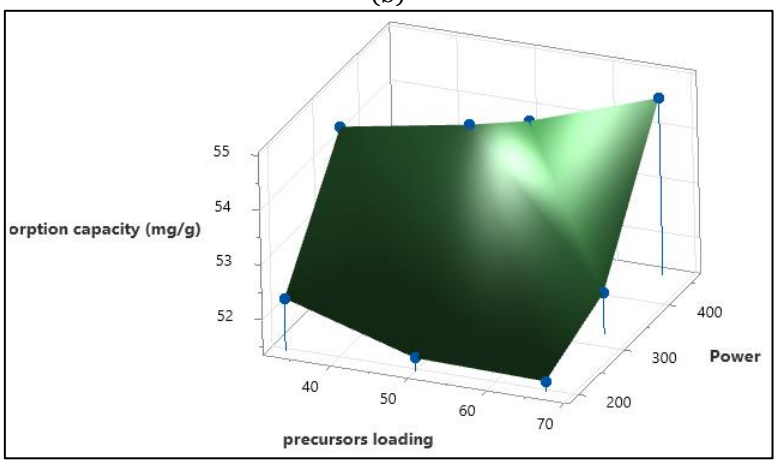

(c)

Fig.6 3D Surface Plots for Adsorption Capacity of Diesel vs (a) pH, Power, (b) pH, Precursors Loading wt.%, and (c) Power, Precursors Loading wt.%.

4.CONCLUSIONS

The main conclusions of the present study could be summarized as follows:

- A novel and direct method to evaluate the optimal conditions of preparation MgO/Fe3O4/AC adsorbent for the selective target of oil removal from oil/water emulsion using the Taguchi method.
- The adsorbent characterization confirms loading MgO and Fe3O4 on an activated carbon surface with a large surface area of 345 m^2/g under optimum preparation parameters to fit maximum oil adsorption capacity.
- The optimum preparation parameters values were an ultrasonic power of 325 Watt, a pH of 10, and a precursor loading weight percentage of 50%.
- The Taguchi analysis for oil adsorption capacity response at a larger S/N ratio was better and showed that pH was the most influential factor in the process, followed by ultrasonic power and precursors loading wt.%.

- The maximum adsorption capacity of 54.8 mg/g for oil was achieved by optimizing the coprecipitation preparation parameters. These results are more comprehensive than those of previous researchers [33].

ACKNOWLEDGEMENTS

The authors are grateful for the financial support for this research from the Chemical Engineering Department, College of Engineering, Basrah University. Postgraduate Research Grant (PGRG) /2022 /Ataa/ENG/39 (988-7-3).

NOMENCLATURE

c_e	Oil concentration at equilibrium, mg/l
c_i	Initial oil concentration, mg/l
m	Mass of adsorbent, g
n	The numbers of runs
q_e	Adsorption capacity(mg/g)
SN_L	Signal to noise ratio
t	Time of reaction, minute
T	Temperature, ℃
v	Volume of sample, l
Wt.%	precursors loading based on Mg
Y_i	The response of each experiment at the i_{th} run

REFERENCES

[1] Yousef R, Qiblawey H, El-Naas MH. **Adsorption as a Process for Produced Water Treatment: A Review.** *Processes* 2020; **8**(12): 1657, (1–22).

[2] Costa TC, Hendges LT, Temochko B, Mazur LP, Marinho BA, Weschenfelder SE, Florido PL, da Silva A, Ulson de Souza AA, Guelli Ulson de Souza SMA. **Evaluation of the Technical and Environmental Feasibility of Adsorption Process to Remove Water Soluble Organics from Produced Water: A Review.** *Journal of Petroleum Science and Engineering* 2022; **208**: 109268.

[3] Klemz AC, Damas MSP, González SYG, et al. **The Use of Oilfield Gaseous Byproducts as Extractants of Recalcitrant Naphthenic Acids from Synthetic Produced Water.** *Separation and Purification Technology* 2020; **248**: 117123.

[4] Fathy M, El-Sayed M, Ramzi M, Abdelraheem OH. **Adsorption Separation of Condensate Oil from Produced Water Using ACTF Prepared of Oil Palm Leaves by Batch and Fixed Bed Techniques.** *Egyptian Journal of Petroleum* 2018; **27**(3): 319–326.

[5] Jiménez S, Micó MM, Arnaldos M, Medina F, Contreras S. **State of the Art of Produced Water Treatment.** *Chemosphere* 2018; **192**: 186–208.

[6] Alomar TS, Hameed BH, Usman M, Almomani FA, Abbad Ba MM, Khraisheh M. **Recent Advances on the Treatment of Oil Fields Produced Water by Adsorption and Advanced Oxidation Processes.** *Journal of Water Process Engineering* 2022; **49**: 103034, (1-26).

[7] Okiel K, El-Sayed M, El-Kady MY. **Treatment of Oil–Water Emulsions by Adsorption onto Activated Carbon, Bentonite and Deposited Carbon.** *Egyptian Journal of Petroleum* 2011; **20**(2): 9–15.

[8] Albatrni H, Qiblawey H, Almomani F, Adham S, Khraisheh M. **Polymeric Adsorbents for Oil Removal from Water.** *Chemosphere* 2019; **233**: 809–817.

[9] Ewis D, Benamor A, Ba-Abbad MM, Nasser M, El-Naas M, Qiblawey H. **Removal of Oil Content from Oil-Water Emulsions Using Iron Oxide/Bentonite Nano Adsorbents.** *Journal of Water Process Engineering* 2020; **38**: 101583, (1-11).

[10] Khurshid H, Mustafa MRU, Rashid U, Isa MH, Ho YC, Shah MM. **Adsorptive Removal of COD From Produced Water Using Tea Waste Biochar.** *Environmental Technology and Innovation* 2021; **23**: 101563.

[11] Mottaghi H, Mohammadi Z, Abbasi M, Tahouni N, Panjeshahi MH. **Experimental Investigation of Crude Oil Removal from Water Using Polymer Adsorbent.** *Journal of Water Process Engineering* 2021; **40**: 101959, (1-11).

[12] Aabid AA, Shakir IK. **Electrocoagulation Coupled Fenton Process for Treating Refinery Wastewater Using a Cylindrical Design of Ti and Al Electrodes.** *Tikrit Journal of Engineering Sciences* 2023; **30**(4): 19–27.

[13] Santos TM, de Jesus FA, da Silva GF, Pontes LAM. **Synthesis of Activated Carbon from Oleifera Moringa for Removal of Oils and Greases from the Produced Water.** *Environmental Nanotechnology, Monitoring and Management* 2020; **14**: 100357.

[14] Ali SJ, Hussain TH, Naje AS, Ajeel MA. **Activated Carbon Prepared from Moringa Husks for Treatment of Oil Field Produced Water.** *Pollution Research* 2020; **39**(2): 240–247.

[15] Hariani PL, Faizal M, Ridwan, Marsi SD. **Removal of Procion Red MX-5B From Songket's Industrial Wastewater in South Sumatra Indonesia Using Activated Carbon-Fe3O4 Composite.** *Sustainable Environment Research* 2018; **28**(4): 158–164.

[16] Malini K, Selvakumar D, Kumar NS. **Activated Carbon from Biomass: Preparation, Factors Improving Basicity and Surface Properties for Enhanced CO2 Capture Capacity - A Review.** *Journal of CO2 Utilization* 2022; **67**: 102318.

[17] James A, Yadav D. **Valorization of Coconut Waste for Facile Treatment of Contaminated Water: A Comprehensive Review (2010–2021).** *Environmental Technology & Innovation* 2021; **24**: 102075.

[18] El-Naas MH, Al-Zuhair S, Alhaija MA. **Removal of Phenol from Petroleum Refinery Wastewater Through Adsorption on Date-Pit Activated Carbon.** *Chemical Engineering Journal* 2010; **162**(3): 997–1005.

[19] Asenjo NG, Álvarez P, Granda M, Blanco C, Santamaría R, Menéndez R. **High Performance Activated Carbon for Benzene/Toluene Adsorption from Industrial Wastewater.** *Journal of Hazardous Materials* 2011; **192**(3): 1525–1532.

[20] Bergmann CP, Machado FM. **Carbon Nanomaterials as Adsorbents for Environmental and Biological Applications.** 1st ed., USA: Springer Nanomaterials for Environmental Protection; 2015.

[21] Fröhlich AC, Foletto EL, Dotto GL. **Preparation and Characterization of NiFe2O4/ Activated Carbon Composite as Potential Magnetic Adsorbent for Removal of Ibuprofen and Ketoprofen Pharmaceuticals from Aqueous Solutions.** *Journal of Cleaner Production* 2019; **229**: 828–837.

[22] Zhou K, Li L, Ma X, Mo Y, Chen R, Li H, Li H. **Activated Carbons Modified by Magnesium Oxide as Highly Efficient Sorbents for Acetone.** *RSC Advances* 2018; **8**(6): 2922–2932.

[23] Zhou K, Ma W, Zeng Z, Ma X, Xu X, Guo Y, Li H, Li L. **Experimental and DFT Study on the Adsorption of VOCs on Activated Carbon/Metal Oxides Composites.** *Chemical Engineering Journal* 2019; **372**: 1122–1133.

[24] Chowdhury A, Kumari S, Khan AA, Chandra MR, Hussain S. **Activated Carbon Loaded with Ni-Co-S Nanoparticle for Superior Adsorption Capacity of Antibiotics and Dye from Wastewater: Kinetics and Isotherms.** *Colloids and Surfaces A: Physicochemical and Engineering Aspects* 2021; **611**: 125868.

[25] Allahkarami E, Dehghan MA, Silva LFO, Dotto GL. **Lead Ferrite-Activated Carbon Magnetic Composite for Efficient Removal of Phenol from Aqueous Solutions: Synthesis, Characterization, and Adsorption Studies.** *Scientific Reports* 2022; **12**(1): 1–16.

[26] Juang RS, Yei YC, Liao CS, Lin KS, Lu HC, Wang SF, Sun AC. **Synthesis of Magnetic Fe3O4/Activated Carbon Nanocomposites with High Surface Area as Recoverable Adsorbents.** *Journal of the Taiwan Institute of Chemical Engineers* 2018; **90**: 51–60.

[27] Guo F, Jiang X, Li X, Jia X, Liang S, Qian L. **Synthesis of MgO/Fe3O4 Nanoparticles Embedded Activated Carbon from Biomass for High-Efficient Adsorption of Malachite Green.** *Materials Chemistry and Physics* 2020; **240**: 122240.

[28] Esmaeili H, Mousavi SM, Hashemi SA, Chiang WH, Ahmadpour AS. **Activated Carbon@MgO@Fe3O4 as an Efficient Adsorbent for as (III) Removal.** *Carbon Letters* 2021; **31**(5): 851–862.

[29] Ingle PK, Attarkar K, Rathod VK. **Ultrasound Assisted Chemical Activation of Peanut Husk for Copper Removal.** *Green Processing and Synthesis* 2019; **8**(1): 46–53.

[30] Park JH, Hwang RH, Yoon HC, Yi KB. **Effects of Metal Loading on Activated Carbon on Its Adsorption and Desorption Characteristics.** *Journal of Industrial and Engineering Chemistry* 2019; **74**: 199–207.

[31] Kaur J, Kaur M, Ubhi MK, Kaur N, Greneche JM. **Composition Optimization of Activated Carbon-Iron Oxide Nanocomposite for Effective Removal of Cr(VI) Ions.** *Materials Chemistry and Physics* 2021; **258**: 124002.

[32] Huang X, Zhang J, Wang W, Sang T, Song B, Zhu H, Rao W, Wong C. **Effect of pH Value on Electromagnetic Loss Properties of Co–Zn Ferrite Prepared via Coprecipitation Method.** *Journal of Magnetism and Magnetic Materials* 2016; **405**: 36–41.

[33] Anifah EM, Ariani IK, Hayati RN, Nugraha SA. **Adsorption of Oil and Grease in Wastewater Using Activated Carbon Derived from Sewage Sludge.** *IOP Conference Series: Earth and Environmental Science* 2022; **1098**(1): 012043.